Design, Characterization & Modelling of a CMOS Magnetic Field Sensor

L. Latorre [1,2], Y.Bertrand[1], P.Hazard[3], F.Pressecq[2], P.Nouet[1]

1 LIRMM, UMR CNRS / Université de Montpellier II, Montpellier France
2 CNES, Quality Assurance Delegation, Toulouse, France
3 Schneider Electric, Nanterre, France

Abstract

This paper presents both the design and the characterization of a full CMOS magnetic field sensor. As an alternative to Hall effect sensors, it acts as a microscopic cantilever, deformed under the action of the Lorentz's force.

1. Introduction

In a strongly competitive economic environment, system providers are continuously looking for new technological solutions to decrease production costs. Recent trends in the technology of VLSI CMOS circuits lead both IC (Integrated Circuit) designers and system providers to add more and more functions to a single ASIC (Application Specific Integrated Circuit). In that way, it seems interesting to implement a sensing element directly on the die where electronic parts have been previously processed [1,2].

Using a CMOS wafer with electronic parts on it, several techniques can be used to implement sensors. Front-Side Bulk Micromachining (FSBM) can be associated or not with Back-Side Bulk Micromachining (BSBM) and sacrificial or extra layer techniques. As the cost of the post-process is strongly affected by the needs for alignment, FSBM seems to be a very promising technique due to its self-alignment capability. This technique is largely available in France through CMP service [3,4].

Concerning magnetic field sensors, a great number of products are commercially available, some of them are associated on the same substrate with electronic parts. In general, these sensors rely on physical principles such as magneto-transistors or magneto-resistors. Although manufacturing technologies have considerably evolved [5], one reproaches often to these sensors a low sensitivity, high power consumption and a high sensitivity to temperature.

In this paper we present a complete methodology that allows to fully characterize electro-mechanical properties of beams realized in a CMOS process. The post-process is first described. Then, the principle of operation of the sensor is exposed and sensor modelling is described. Measurement results are finally presented so as to compare expected performances with current products and to propose the design of a monolithic magnetic field sensor.

2. Sensor manufacturing

Sensor design and manufacturing is performed into independent steps. First, a CMOS circuit foundry is used to provide dies according to designer requirements and then wet etching of those dies is realized.
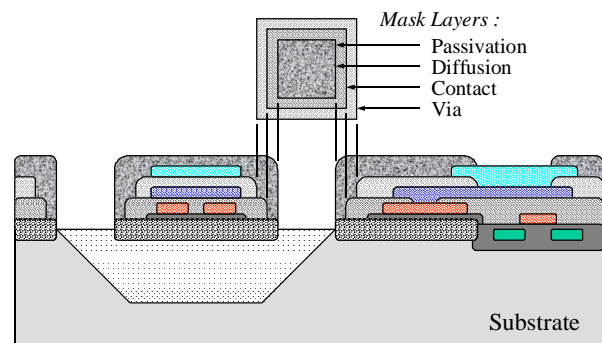

Figure 1: CMOS manufacturing process and associated post-process.

Figure 1 represents a cross-sectional view of a CMOS process. During the standard CMOS process, polysilicon metal and oxide layers are deposited above a substrate. According to designer requirements several etching masks can be superimposed to leave uncovered silicon bulk at the end of the standard CMOS process. Then, post-process operates as an anisotropic silicon etching

that uses the various oxide layers as natural mask. <100> substrate planes can then be etched leaving the <111> planes of the silicon substrate. Suspended structures such as cantilever beams, bridges or membranes are then obtained. Fabless designers can easily address this technology and low development costs are expected due to the re-use of the same technology for various physical phenomena.

3. Characterization and modelling

Suspended structures are mainly constituted with silicon oxides. According to its needs, the designer can add polysilicon or aluminum layers. Polysilicon is used to realize piezoresistive strain gauges while in our case aluminum is used to implement a current loop in order to obtain the Lorentz's force. Unfortunately, electromechanical and mechanical properties of such materials are not so well known than electrical ones. It is therefore indispensable to undertake a preliminary characterization job.

3.1. The "U-Shape" cantilever device

Our characterization approach is based on the experimental result comparison with a theoretical 2nd order mechanical model. Figure 2 represents a photograph of one of the studied device. It concerns a "U-shape" cantilever beam which is particularly suitable for Lorentz's force actuation. It is formed with two parallel cantilever beams that are connected at their free extremity by a "linking arm". The associated mechanical model is a classical second order model where k, M and D represent respectively the stiffness, the mass and the damping factor of the structure.
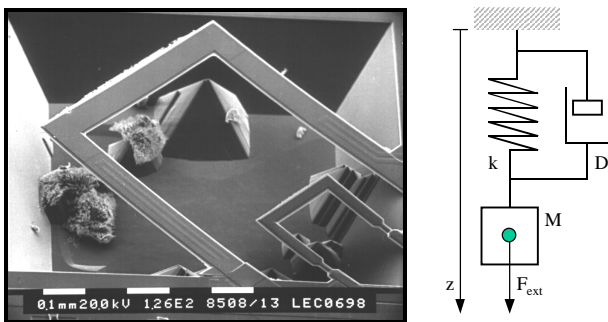
$$M \frac{d^2 x}{dt^2} = -k(x - x_0) - D \frac{dx}{dt} + F_e$$

Figure 2: SEM photograph of a «U-shape» cantilever and associated mechanical model

3.2. Magnetic field actuation and detection

Assuming that the beam is flowed by an electrical current (the force current) and is placed in a magnetic field as described in figure 3, the free length of the beam is submitted to a force. The subsequent deformation is then electrically translated thanks to the strain gauges situated at the clamped end of both suspension arms.
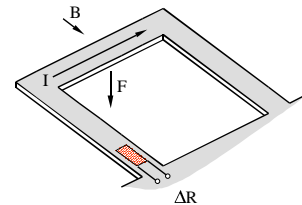

Figure 3: Magnetic field actuation principle

The generated force can be either static or dynamic depending on the nature of both magnetic field and force current. For characterization purposes it is also possible to assign a vertical displacement to the center part of the "linking arm" using a micrometric screw. The vertical force (F) is then unknown but can be directly deduced from $F = k \cdot z$ where k is the equivalent stiffness of the whole device.

3.3. Electromechanical modelling

Each structure consists in an heterogeneous stack of various process layers, namely silicon oxides, metals, polysilicon and passivation nitride. The sensing capability of such a device comes from the piezoresistivity of the polysilicon layer. To provide simulation models for designers we have first developed analytical expressions for mechanical parameters (k, M and D). Basic mechanical relations (Figure 4) are used to calculate those parameters with the following inputs:
- geometrical data (from mask drawing),
- data from manufacturing process (e.g. deposited thickness),
- densities and Young's modulus of materials [6].

The complete electromechanical model will take into account the stress magnitude in polysilicon gauges. Thus, in associating this stress calculation with experimental measurements of the gauge resistance at calibrated forces, it is then possible to estimate the polysilicon gauge factor. The main difficulty of the stress estimation concerns the heterogeneous composition of the beam section. Figure 5 shows a simplification method, whose principle lies in the normalization of each layer width with respect to its Young's modulus [7].
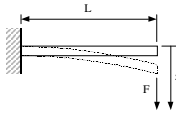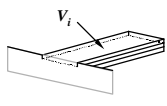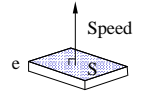
K	M	D
$k = \dfrac{F}{z} = \dfrac{3 E_n I_n}{L^3}$ E_n : Young's modulus I_n : Moment of inertia	$M = \sum_i d_{i_n} \times V_{i_n}$ d_i : Density V_i : Volume	$D = \dfrac{S}{e} \mu_{air}$

Figure 4: Mechanical parameters and associated models

From the so obtained shape, the moment of inertia (I_n) of the beam can be easily calculated together with the position of the neutral fiber of the beam. The deduced homogeneous section is then mechanically equivalent to the original heterogeneous one. The complete analytical model has been translated in Analog HDL language, what authorizes simulations in a microelectronic designer framework. This electromechanical model is finally composed with:

- the transfer function between magnetic field and force as defined in section 3.2,
- the conversion between a force applied at the free extremity of the "U-shape" cantilever and a vertical displacement (section 3.1) including processing of k, M and D deduced from design parameters and figure 4 relationships,
- the calculation of the average stress in each gauge for a given vertical displacement and the associated resistance variation using the gauge factor of the polysilicon layer [8].

As an example, Figure 6 shows a comparison between measured and simulated frequency response for a "U-shape" cantilever device. The accuracy of the simulated data remains within 10 percent of silicon data. This is sufficient if we compare with the uncertainty on process parameters such as horizontal and vertical dimensions or Young's modulus. In that way the common idea consisting in making highly time consuming finite element simulations on mechanical structures defined with geometrical and physical uncertainties in the 20 percent range lost a lot of sense.
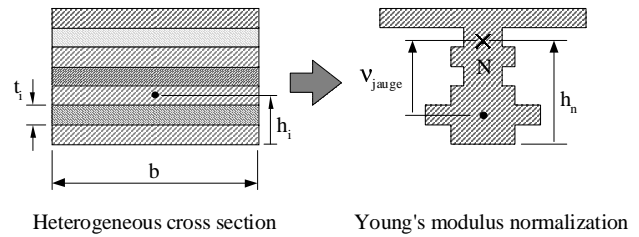

Heterogeneous cross section   Young's modulus normalization

Figure 5: Normalization process of the heterogeneous section

3.4. Sensor characterization results

The device described on Figure 2 has been experimentally studied in different situations:

- with a constant magnetic field and a dynamic force current flowing into the beam (crosses on figure 6),
- with a static displacement imposed on the beam extremity (figure 7),
- at the resonant frequency with various magnetic field magnitudes (figure 8),
- without any magnetic field and with various DC force current flowing through the beam (figure 9).

The frequency-domain response is consistent with a second order system. The obtained Q-factor is about 70. On smaller structures figures up to 100 have been reached. According to the resonant frequency response, one obtains for a Wheatstone bridge and a power supply of 5 volts, a sensitivity of 300mV/T with a current consumption of 40mA. The power consumption can easily be reduced by one order of magnitude by increasing the number of current loops in the structure. Currently fixed to 1 for characterization purposes, it can be increase easily up to 10 in order to obtain the same behavior with a lower force current. These performances are then comparable to those of Hall effect sensors.
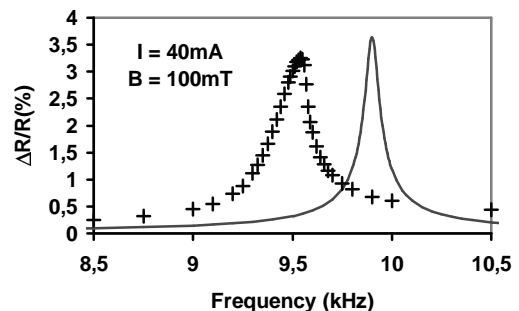

Figure 6: Frequency-domain behavior (measured and computed)

The static behavior exhibits a strong linearity over a broad range. Considering the elastic nature of the structure, one can consider that the gauge resistance variation is directly proportional to the displacement of the free extremity of the beam.
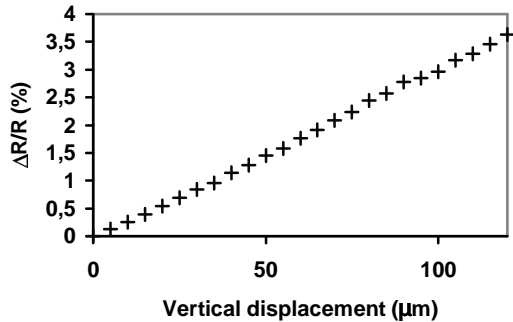

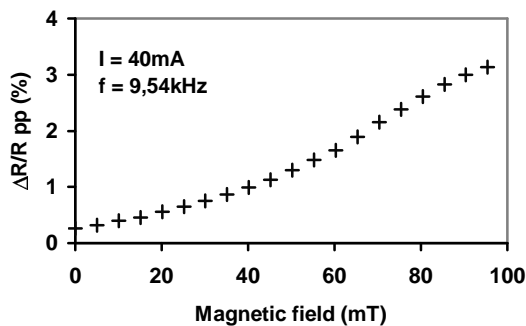**Figure 7: Resistance variation versus vertical displacement of the beam extremity**

Figure 8: « resonant » response versus magnetic field magnitude
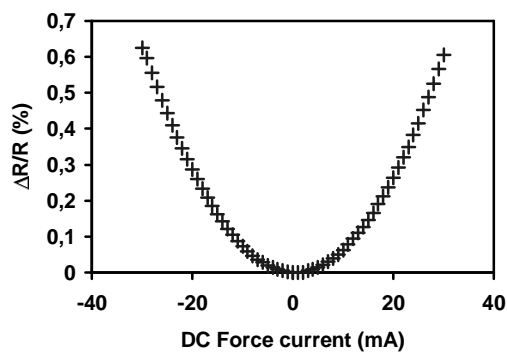

Figure 9 : Effect of force current on gauge resistance

Gauge resistance value changes with force current (figure 9). This phenomenon can be associated with the beam heating due to Joule effect of the DC current force.

The obtained time constant is large and then this variation is completely filtered when the force current is applied at the structure resonant frequency. Using two identical U-shape cantilevers activated in a phase opposition manner leads to a full Wheastone bridge with four gauges. It is then possible to increase the sensitivity of the sensor by a factor 4 (i.e. 1.2V/T). In this case temperature effect are also compensated.

About noise, no characterization results are available at the moment but some positive points can be mentioned:
- the thermal noise into gauges is known to be low,
- using the sensor in resonant mode, result in shifting the signal around resonant frequency, where spectral density of the 1/f noise is the lowest,
- the sensor in resonant mode is a very selective band-pass filter. Thus, the RMS value of noise which is proportional to the width of the band-pass filter is reduced. In this case, the SNR should be interesting.

4. Sensor integration

A two-cantilever sensor and two simple-cantilever sensors were integrated with an amplifier stage of gain 50 in order to reach a full-scale output of 5V under a magnetic field of 100mT. Simulations of both mechanical parts and electronic parts have been performed using analog models previously presented.
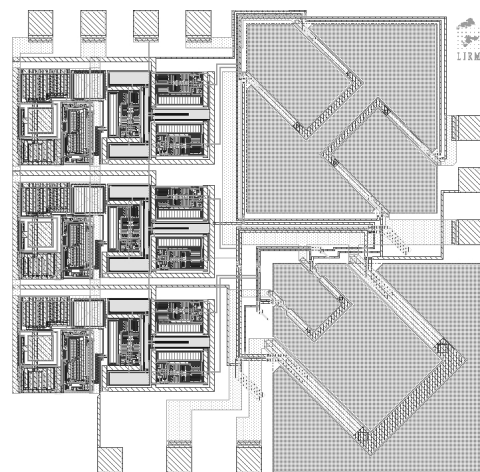

Figure 9 : Layout of the final sensor

The layout of the circuit is presented on figure 10. It's a square of 5 mm^2 in size with equilibrium between mechanic and electronic parts. Circuit manufacturing has been realized by AMS on a 0.8 μm CMOS technology available as multiproject wafer through CMP services [3,4]. Post-process is currently under achievement using

TMAH solution by a small company, Ion Beam Services in Rousset, France.

5. Conclusion

Several aspects condition the use of Micro-Electro Mechanical Sensors (MEMS). Among them the global cost (both for technology and products) and reliability (short and long terms) play a major role. Our approach focuses on low-cost MEMS obtained by processing chips issued from an industrial CMOS process.

Such a technique allows implementing both sensing and electronic parts on the same chip. Integrating the whole conditioning/processing chain gives the opportunity of precociously digitizing the analog signal issued from the sensor thus enhancing the noise immunity of the system. Finally, this technique easily allows the addition of Built-In Self-Test and/or on-chip self-calibration facilities. In this paper, we have introduced a complete methodology for the characterization, modelling and design of a magnetic field micro-sensor fully integrated on a silicon substrate. CMOS compatibility and batch compatible post-process insures low production costs.

A first prototype including on the same die sensing and electronic parts has been designed and post-manufacturing results will allow to state on the performances of such a technology.

6. References

[1] H. Baltes, IC MEMS Microtransducers, Tech. Digest, IEEE Int. Electron Devices Meet., 1996, pp. 521-524.

[2] H. Baltes and al., Thermomechanical microtransducers by CMOS technology combined with micromachining, Micro System Technologies 91, 1991, pp. 98-103.

[3] Information is available on the World Wide Web at the following address: http://tima-cmp.imag.fr/tima/mcs/mcs.html

[4] J.M. Karam, B. Courtois, J.M. Paret "Microelectronics Compatible Manufacturing Techniques of Microsystems", Mechatronics ' 96

[5] C.S. Roumenin, "Magnetic sensors continue to advance towards perfection", Sensors and Actuators A, Vol 46-47, pp. 273-279, 1995

[6] K.E. Petersen, "Silicon as Mechanical Material" Proceedings of IEEE, Vol 70, pp. 420-457, 1982

[7] S.P. Timoshenko, "Strength of Materials", D. Van Nostrand Inc., Princeton New Jersey, 1968.

[8] L. Latorre, Y. Bertrand, P. Nouet, "On the use of Test Structures for the Electromechanical characterization of a CMOS compatible MEMS technology", Proc. IEEE 1998 Int. Conf. On Microelectronic Test Structures, March, 1998.